BILINGUAL PUBLISHING CO.
Pioneer of Global Academics Since 1984

Journal of Geographical Research
https://ojs.bilpublishing.com/index.php/jgr

ARTICLE

The Use of Airborne LiDAR in Assessing Coastal Erosion in the Southeastern USA

David F. Richards IV[1*] Adam M. Milewski[1] Brian Gregory [2]

1. Water Resources & Remote Sensing Lab (WRRS), Department of Geology, University of Georgia, Athens, GA 20602, USA
2. Southeast Coast Inventory & Monitoring Network (SECN), Main Office, Southeast Coast Network, Athens, GA 30605, USA

ARTICLE INFO

Article history
Received: 31 May 2022
Revised: 01 July 2022
Accepted: 11 July 2022
Published Online: 02 August 2022

Keywords:
Coastal
Erosion
LiDAR
Elevation
Volumetric change
Geomorphology
Sea level

ABSTRACT

Changes in sea level along the coastal southeastern United States (U.S.) influence the dynamic coastal response. In particular, the Southeast Coastal Network (SECN) of the National Park Service (NPS) has exhibited evidence of fluctuations in sea level which caused coastal erosion. Airborne LiDAR acquired from NOAA for Fort Matanzas National Monument, Fort Pulaski National Monument, Charles Pinckney National Historic Site, and Cape Lookout National Seashore were analyzed to identify changes in both elevation and the spatial volume of unconsolidated sedimentary material in the coastal southeast over time. Areas that exhibited an increase (deposited material) or decrease (eroded material) in elevation were mapped across the study area from 2006 to 2018. Results indicate a quasi-cyclic process where unconsolidated sediment distribution and the morphodynamic equilibrium changes with time. The coastal zones are steadily oscillating between the process of erosion and deposition affecting the coastal geomorphological dynamic. The use of LiDAR for evaluating coastal sustainability and resiliency due to this environmental phenomenon is clear.

1. Introduction

The coastal southeast United States (U.S.) is highly susceptible to geomorphological and hydrogeological changes in response to relative sea level rise. Climate change increases both the quantity and intensity of storms which results in subsequent sea level rise [1-3]. Many variables play a role in the geomorphological and hydrological response to this shift. These variables are intrinsically connected, defining the interaction and link of hydrologic and geomorphic processes in both temporal and spatial dimensions [4,5]. The Atlantic Coastal Plain is extremely sensitive to sea level rise, causing accelerated erosion

*Corresponding Author:
David F. Richards IV,
Water Resources & Remote Sensing Lab (WRRS), Department of Geology, University of Georgia, Athens, GA 20602, USA;
Email: milewski@uga.edu

DOI: https://doi.org/10.30564/jgr.v5i3.4762

rates and changes in the amount of sediment deposited in coastal areas [6-8]. As this is representative of the hydrogeological impact, the economic impacts are analogous to the direct damages of sea level rise [9-11].

Global mean sea level rise has risen about 21 centimeters ~ 24 centimeters (0.21 meters ~ 0.24 meters) since 1880, with about a third of that coming in just the last two and a half decades [12]. By 2100, research suggests that sea level rise could exceed 2 meters, given the climate regimes continue at their current rates [13]. Along the southeastern US coastline, approximately 43% (~2,000 km) of the area is projected to have an increase in coastal erosion vulnerability by the 2030s, with respect to its present vulnerability [14]. Studies have shown that the coastal sediment budget, representing the sediment supply, is extremely vulnerable [15-17]. Coastal erosion is continuously altering the environment and mitigating its effects has become increasingly important. To meet the increasing demand for coastal resource management, remote sensing techniques are being used to provide rapid data acquisition of large areas that would normally require extensive and lengthy field surveys. Furthermore, the ability to use light detection and ranging (LiDAR) in both natural resource management and economic sustainability, creates the opportunity to distinctively characterize the coastal dynamic response at high spatial resolutions.

Typically, LiDAR is used in forest management to understand biomass dynamics as it was historically believed to show the greatest promise over these areas, however, its use in coastal applications has become a pivotal tool in coastal change detection [18,19]. The ability of LiDAR has garnered efficient, productive, and accurate measurements of topographical mapping [20-22]. LiDAR's application enables rapid elevation data collection through repeated measurements of the observed topographic region [23]. The high spatial resolution data retrieved produce digital elevation models (DEMs) indicative of current and historical coastal geomorphological changes. The results have become an asset in improving the knowledge of complex coastal geomorphological processes creating better preventative and mitigating initiatives [24-26].

In recognition of the changes occurring along the coastal southeast US, the sediment budget has displayed both aggraded and degraded material [27,28]. In this paper, we present the use of LiDAR in characterizing the spatial and temporal changes of the coastal southeast US, and quantify these changes at select National Park sites. More specifically to identify the temporal changes in elevation, and quantify the spatial volumetric changes of unconsolidated sedimentary material in the Southeastern Coastal Network (SECN) of the National Park Service (NPS).

In the acquisition of temporal LiDAR of SECN NPS sites, land cover data is used to represent the topographic features of the coastal southeast US through ArcGIS and ENVI LiDAR. The final outputs are presented in a GIS framework, providing a volumetric spatial change analysis detailing the specific areas where the erosional activity occurred (net loss) and where unconsolidated material was returned to the environment (net gain). This high-resolution LiDAR data not only exhibits the advantages of LiDAR to improve coastal water resources and the understanding of the coastal geomorphologic dynamic, but also its applicability in providing sustainability and resiliency of environmental change.

2. Study Area

The SECN of the NPS monitors seventeen national parks extending along the Atlantic coast from the North Carolina-Virginia border to Cape Canaveral, Florida providing natural resource management. The areas used in this study are Fort Matanzas National Monument (NM) in St. Augustine, Florida, Fort Pulaski National Monument (NM) in Savannah, Georgia, Charles Pinckney National Historic Site (NHS) in Sullivan's Island, South Carolina, and Cape Lookout National Seashore (NS) in Harkers Island, North Carolina. The areas used for Fort Matanzas NM and Cape Lookout NS are within the SECN site boundaries, while the areas used for Fort Pulaski NM and Charles Pinckney NHS are in the vicinity of the SECN site boundary. These sites were selected as each is representative of the states in a longitudinal context along the southeastern US coastline covering 959 km (959,000 m). The distance between each site location is as follows: Fort Matanzas NM to Fort Pulaski NM is 312 km (312,000 m), Fort Pulaski NM to Charles Pinckney NHS is 189 km (189,000 m) and Charles Pinckney NHS to Cape Lookout NS is 468 km (468,000 m). The climate within this region can be categorized as humid subtropical where a wide range of extreme weather and climate events persist [29,30]. The El Niño Southern Oscillation (ENSO) is key to understanding the interannual variations of the climate of the SECN. El Niño will usually have lower temperatures in winter and spring, increased winter precipitation, and fewer tropical systems [30]. Mean annual precipitation in the SECN is mostly consistent, however, precipitation increases towards the Atlantic coast. In each of the SECN NPS sites the mean annual precipitation is between 1,001-1,400 millimeters (mm)/year [30]. Along the Atlantic coastline precipitation is more present during the summer months. Temperatures in the SECN vary largely as a function of latitude and proximity to the coast. Mean annual temperatures are between 14.1 °C to 24 °C [30]. The tem-

peratures are higher in the southern states and lower in the northern states. Winter temperatures show a strong latitudinal gradient, while summer temperatures are moderate along the coast but warmer inland. Although the proximity of oceans generally moderates extreme temperature conditions with average summertime maximum temperatures around 30 °C, daytime temperatures can occasionally reach 40 °C [30].

Each of the sites is in the Atlantic Coastal Plain geological province, where geomorphologic changes have occurred [31]. Fort Matanzas NM is located in the Southeastern Coastal Plain geologic province, specifically in the east central Floridan aquifer system (Figure 1). Within the site are saltwater marshes and freshwater wetlands underlain by a surficial aquifer, confining unit and the upper Floridan aquifer [32,33]. The surficial aquifer varies seasonally while containing sands, marl, peats, mud, and alluvium [33,34]. The upper Floridan aquifer contains materials from the Eocene to Miocene, where the Hawthorn, Suwanee limestone and Ocala limestone formations are present [33]. Separating the surficial aquifer from the upper Floridan aquifer unit is an unconformity where the Hawthorne formation is above the Suwannee limestone [35]. The Hawthorn formation contains interbedded sand, phosphatic clay, dolomite, and limestone [33]. Within the Suwannee limestone, silt and clay are present [33]. The Ocala limestone is separated by an upper and lower lithological unit. The upper member is a marine limestone with coquina and chert, whereas the lower member is a marine limestone with dolomite [33].

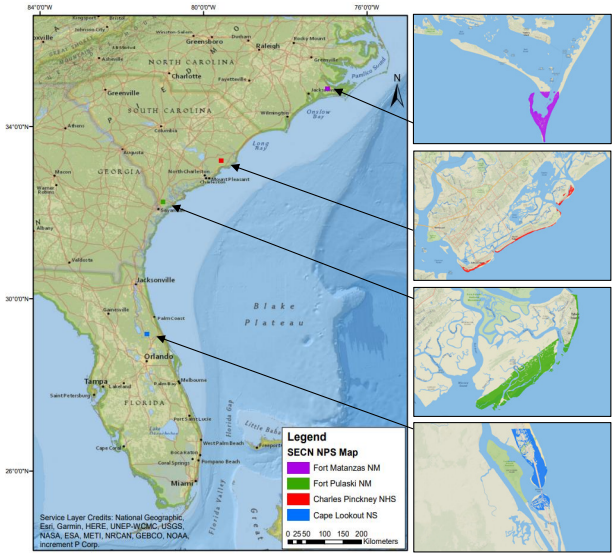

Figure 1. GIS-derived map of Fort Matanzas NM, Fort Pulaski NM, Charles Pinckney NHS, and Cape Lookout NS locations.

Fort Pulaski NM is located within the Atlantic Coastal Plain geologic province lying at the bottom most region of the Savannah River, which consist of salt marshes and hummocks (Figures 1 and 2). This site is composed of sand, peat, alluvium, unconsolidated material, clay, and beach sand [36]. Most of the material is of carbonates, while the younger rocks are clastic with limestone present near the surface and traces of glauconite underneath the limestone [36]. These materials are of the Late Cretaceous to Holocene with rocks of early Eocene to Oligocene [36]. The sands are of the Satilla, Coosawhatchie, and Marks Head formations [37]. The Satilla Formation immediately underlies the land surface where it is composed of sand, clay, and silt deposited in shallow marine environments [38,39]. The Coosawhatchie Formation is mostly comprised of silty clay, clay diatomite and phosphate sands [37,40]. These materials persist heavily, thus, they are divided into individual sedimentary units. The five-unit members are Tybee Phosphorite, Meigs, Berryville Clay (upper) Berryville Clay (lower) and Ebenezer formations [39]. In the Marks Head formation is predominantly of medium to coarse phosphate-calcareous sands [39,41]. These formations are in the Upper and Lower Floridan carbonate aquifer system where the layers are of limestone and dolomite [37]. The Upper and Lower Brunswick aquifers are present in this region [36]. The upper Brunswick aquifer is home to the Marks Head and members of Coosawhatchie formations. The confining unit with the surficial aquifer above contains other members of the Coosawhatchie formation except for the Ebenezer formation [37].

Charles Pinckney NHS is in the Atlantic Coastal Plain geologic province of South Carolina (Figure 1). In this region there are layers of surficial aquifer systems that are separated by an unconfined upper surficial aquifer composed of artificial till and a partially to fully confined lower surficial aquifer composed of sands [42]. Specifically, this site is underlain by confining units, Black Creek, Middendorf, and Cape Fear aquifer systems [43]. The confining unit between the Black Creek aquifer and Middendorf aquifer consists of sandy clay material [44]. This lithology is similar in the confining unit between the Middendorf and Cape Fear aquifers. Black Creek's aquifer unit is composed of fine to medium sand where the aquifer's thickness remains constant [45]. The Middendorf aquifer consists of thin, laminated layers of fine to medium sand and clayey material [44]. The layers of clayey material persist in Cape Fear's aquifer unit, but it is separated by sand, silt, and gravel [44].

Cape Lookout NS is a member of the North Carolina Outer Banks, a barrier island within the Atlantic Coastal Plain geologic province (Figure 1). This site is underlain by surficial aquifers with confining units. Yorktown,

Castle Hayne, Beaufort, Peedee, Black Creek, Upper and Lower Cape Dear aquifer systems are composed of marine sediments [46]. The upper confined aquifer is part of the early Pliocene Yorktown Formation which is comprised of sand, partially consolidated shell beds and sandy limestone. Some of these sand and shell beds near the surface of the aquifer are of the Quaternary age [47]. The lower confined aquifer, Castle Hayne, is composed of medium to coarse grained limestone [47]. This aquifer is confined by the Pungo River formation of the early and middle Miocene age, where layers of clay, silty clay, and clayey sand persist [46]. The Pungo River Formation is the highest yielding aquifer in the North Carolina coastal plain [48].

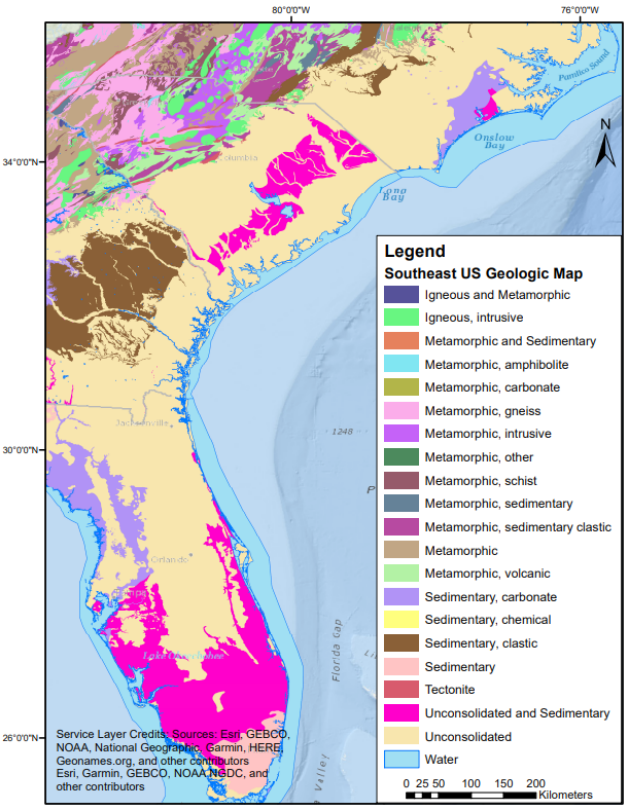

Figure 2. Geologic map of southeast US. Data retrieved from the USGS State Geologic Map Compilation geodatabase of the conterminous United States.

3. Methodology

The methodology implemented in this study incorporates a series of steps designed to synthesize volumetric, spatial, and temporal changes using LiDAR (Figure 3). The LiDAR data acquired were retrieved from the National Oceanic and Atmospheric Administration (NOAA), (https://coast.noaa.gov/dataviewer/#/lidar/search/), in LAS format. The data were collected, categorized, and processed individually for each of the four respective SECN NPS sites. The processed data was used to create a change analysis both spatially and temporally. Using ENVI LiDAR 5.5, each acquired LiDAR dataset generated point clouds, orthophotos and DEMs (horizontal accuracy: 1-meter, vertical accuracy: 0.196 meters) to produce the base maps. From the production of the temporal LiDAR base maps detailing changes in elevation, the data were then used to provide a volumetric spatial change analysis. The volumetric spatial change analysis was used to detail specific areas where the erosional activity occurred (net loss) and where unconsolidated material was returned to the environment (net gain). Using the spatial analyst tool, the raster calculator calculated the difference from each year to generate a difference map. The difference maps were then edited by the Cut Fill tool to display the volumetric changes that were quantified and measured to visually represent the net gain/net loss of unconsolidated material.

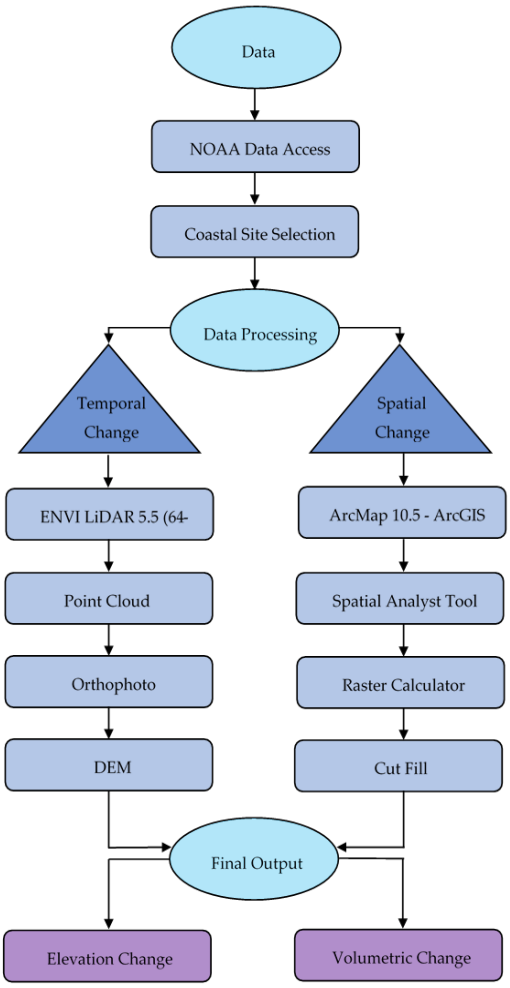

Figure 3. Processing flow chart representing data acquisition, processing procedure, and final output of the LiDAR dataset. Each step in this series was used to display the temporal changes over the specified period and the spatio-temporal volumetric changes.

3.1 Data Acquisition

Before the LiDAR acquisition, the LiDAR system underwent calibration to verify the operational accuracy and misalignment angles. Boresight calibrations were performed for the LiDAR system at the beginning and end of each flight mission. LiDAR data was processed immediately after the acquisition to verify the coverage had no voids. The GPS/Inertia Measurement Unit (IMU) data was post processed using differential and Kalman filter algorithms to produce the best estimates of unknown variables [49].

The vertical and horizontal accuracy was performed using a standard method to compute the root mean square error (RMSE) based on comparing ground control points and filtered LiDAR data points. Each compiled vertical and horizontal accuracy value met the 95th percentile confidence level requirements recommended by the American Society for Photogrammetry and Remote Sensing (ASPRS) when analyzing elevation generated by LiDAR. The horizontal accuracy quantitative value is 1 meter, and the vertical accuracy quantitative value is 0.196 meters (19.6 cm). The ASPRS guidelines follow the National Digital Elevation Program sections on vertical accuracy testing that follows the Federal Geographic Data Committee and the National Standard for Spatial Data Accuracy [49]. The filtered LiDAR data represented the bare earth elevations from 2006 to 2018 for each NPS site (Table 1). The bare earth elevations collected multiple returns x, y, and z data as well as intensity data. This data was then compressed in a LAS binary file format containing the information specific to the LiDAR data (number of returns, intensity value, x, y, z, etc.). The LAS data was projected to input datum NAD83, the projection system was geographic longitude/latitude, and the input units were converted to meters [49]. As a result, the data acquired from NOAA are as follows:

3.2 LiDAR-based DEM Temporal Changes

In the acquisition of temporal LiDAR at each of the SECN NPS sites, land cover data were used to represent the topographic features of the coastal southeast US using ArcGIS and ENVI LiDAR. The topographic features detailed the elevation changes that have occurred at each of the sites.

ENVI LiDAR was used to process the geo-referenced LiDAR point cloud data into geographical information system layers that were then produced in output formats for a 3D visual database. ENVI LiDAR created Digital Elevation Models (DEMs) from the Digital Terrain Models (DTMs) to characterize the elevation of the site's topography. Geospatial measurements of the point cloud data were used to provide accuracy of the existing topographic cover. Each point is classified by a value of elevation height to determine its class feature.

ENVI LiDAR used the DTM to create the DEM by including vector data of the natural terrain and linear features. The vector data are composed of regularly spaced raw points and natural features of the observed area. The linear features used are representative of the shape of the bare-earth terrain. The regularly spaced raw points, vector data and linear features are used to augment a DEM providing its distinctive terrain features. To ensure DEM extraction from LiDAR data based on DTMs was accurate, a density map was generated to check the raw point density and coverage of the LiDAR data. Each of the LiDAR datasets had more than the recommended minimum of 5 to 6 points per square meter by L3 Harris Geospatial. Due to the dense raw dataset, ENVI LiDAR identified features for extraction and avoided false readings including overestimations of topographical features. Usage of Variable Sensitivity Algorithm for low density datasets was not performed.

ArcGIS was used to provide the final output of the processed LiDAR point cloud data in a GIS produced map. The base maps were used to create the different maps, which display the differences in elevation over a specified year. These maps detailed the elevation values of the processed LiDAR points acquired from NOAA. The maps provide a geographical representation of the temporal changes that have occurred over time.

Table 1. LiDAR data details for each NPS site.

Sites											
Fort Matanzas NM			Fort Pulaski NM			Charles Pinckney NHS			Cape Lookout NS		
Value	**Season**	**Year**	**Value**	**Season**	**Year**	**Value**	**Season**	**Year**	**Value**	**Season**	**Year**
0.30 m	Fall	2006	0.30 m	Winter	2006	0.20 m	Winter	2007	0.30 m	Fall	2012
0.20 m	Fall	2010	0.24 m	Winter	2009	0.20 m	Fall	2010	0.10 m	Fall	2014
0.22 m	Winter	2013	0.20 m	Fall	2010	0.23 m	Winter	2016	0.23 m	Winter	2017
0.20 m	Fall	2016	0.23 m	Winter	2016	0.20 m	Fall	2018	0.20 m	Fall	2018
0.20 m	Fall	2017	0.10 m	Winter	2017	N/A	N/A	N/A	N/A	N/A	N/A

3.3 Spatial Change Analysis

The temporal LiDAR base maps provided a volumetric spatial change analysis detailing erosional activity (net loss) and deposition (net gain). To identify the changes occurring spatially, the ArcGIS Cut Fill tool was applied. This tool analyzed topographic features at two different periods to identify the volumetric change by (1) identifying regions of erosional activity and deposition, (2) calculating the volume of sedimentary material, and (3) identifying inundated regions.

The Cut Fill tool displays regions of net loss and net gain from the attribute table of the output raster. Each raster represents a region's volume, which is calculated for each cell, and the area, calculated by the number of cells in each region by the cell size. The volume is greater than zero in regions where the unconsolidated sedimentary material was cut, and less than zero where it was filled. This repeated spatial change analysis identified the erosional and depositional activity that has occurred.

4. Results

Each site analyzed in this study displays the temporal changes in elevation and the quantification of spatial volumetric changes of unconsolidated sedimentary material presented in a GIS framework. The LiDAR-based DEM temporal changes display the highest and lowest elevation for each year at each site. Of the temporal change analysis, the spatial changes occurring were displayed volumetrically to identify the deposited material and erosional activity occurring during specific years at each site.

Fort Matanzas NM, Fort Pulaski NM, Charles Pinckney NHS, and Cape Lookout NS are all depicted to display how each site individually changed temporally and spatially during the specified period time (Figures 4-11, Tables 2-5). Tables 2-5 present the net loss and net gain of the given total area for each output raster's attribute table of the specified year. These tables detail the percentages of erosional and depositional activity that occurred spatially. The temporal changes were characterized by the acquisition of LiDAR derived DEMs for each location (Figures 4, 6, 8, 10). The earliest acquired DEM was selected as the base map to display how elevation changed from the base map's year to each specified year. The spatial change maps were derived from the temporal change maps to represent the volumetric distribution of erosional activity and deposited unconsolidated sedimentary material (Figures 5, 7, 9, 11). These maps display the extent and location of where changes have occurred over the study period. Results show instances of elevation and volumetric changes of sediment though no consistent trend was found.

4.1 Fort Matanzas National Monument

LiDAR derived DEMs of Fort Matanzas NM displays the elevation changes that have occurred from 2006 to 2017. From 2006 to 2010 the elevation dropped a meter and there was a majority net loss of material occurring (Table 2) (Figure 4).

Table 2. Fort Matanzas NM spatial change extent of sedimentary material deposited (net gain) and areas where erosional activity occurred (net loss).

FORT MATANZAS NATIONAL MONUMENT SPATIAL CHANGE ANALYSIS		
	2010	
Total Area (m^2)	59,729	100%
Net Loss	48,497	81%
Net Gain	11,231	19%
	2013	
Total Area (m^2)	104,255	100%
Net Loss	91,590	88%
Net Gain	12,664	12%
	2016	
Total Area (m^2)	102,385	100%
Net Loss	90,863	89%
Net Gain	11,521	11%
	2017	
Total Area (m^2)	100,803	100%
Net Loss	90,279	90%
Net Gain	10,523	10%

From 2006 to 2017, the elevation drops considerably within the middle of Fort Matanzas NM (Figure 4). During 2010 to 2017, the areas of the highest elevations, labeled in red, include the areas around the coastline and some of the inner portions of this coastal environment (Figure 4). As depicted in the images, the coastline is continuously altered as the elevation changes from year to year. From 2010 to 2013 the coastline is at its highest elevation, while from 2016 to 2017 the coastline continues to decrease. Near the Matanzas Inlet you see a consistent decline in elevation from 2010 to 2017. The eastern coastline displays higher elevation values in comparison to the inlet near Rattlesnake Island.

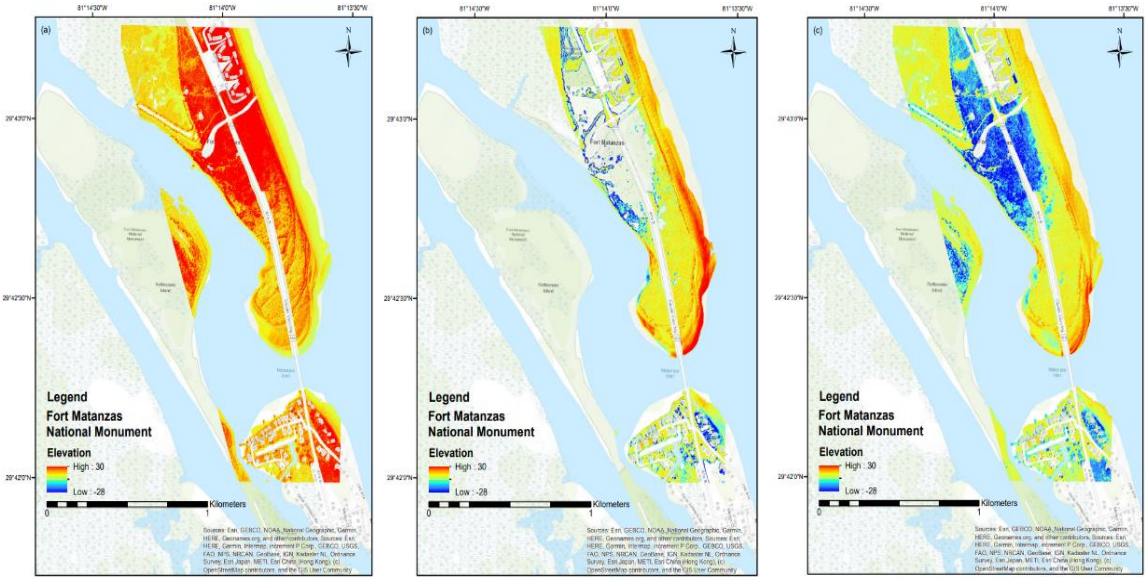

Figure 4. LiDAR derived DEM difference maps generating three-dimensional elevation changes of Fort Matanzas NM from 2006 to 2017. Each panel corresponds to the specified year: (a) 2006, (b) 2010, (c) 2013, (d) 2016, and (e) 2017.

The volumetric change of unconsolidated sedimentary material at Fort Matanzas NM displays a net loss from 2010 to 2017. During this time period, the spatial extent of where the erosional activity occurred increased (Table 2). In 2010, there was a net loss of 81%, while in 2017, the net loss increased to 90% over the given area. Though much of the material displayed is a net loss, there is also a net gain. Outlined by the red color on the volumetric change maps, the eastern coastline shows where much of the sedimentary material was deposited back into the environment representing a net gain (Figure 5). Additionally, there is a net gain of material where tidal inlets are present. According to the spatial change analysis, from 2010 to 2017, there is a decrease in sedimentary material being deposited back into this environment (Table 2).

4.2 Fort Pulaski National Monument

From 2006 to 2017, the area near Fort Pulaski NM exhibited varied changes in elevation. The LiDAR derived DEMs of this coastal environment display how the elevation is fluctuating over a given period of time. From 2009 to 2010, elevation values display an increase towards to southern most region of the site and towards the northeast. In 2016, there is a decrease in elevation in pockets near the southern most region and along the eastern coastline. In 2017, the elevation remains constant (Figure 6). The northernmost and southernmost regions exhibited the highest elevation values in Tybee Island and Little Tybee Island, while the center most regions recorded the lowest elevation values (Figure 6).

The volumetric change maps of this area show an overall net loss of unconsolidated sedimentary material from 2009 to 2017 (Table 3). In 2009, there was a net loss of 85% but the erosional activity that occurred from 2009 to 2010 decreased to 75% over the given area (Figure 6). In 2016 and 2017, there is an increase in unconsolidated sedimentary material with a net loss of 84% (Figure 7). The locations where there is a net gain are similar during this temporal data collection. Material has been deposited back into this environment along the eastern coastline displaying a net gain of material in the tidal inlet between Little Tybee and Tybee Island. The southern region along the coastline displays regions of a net gain where the majority of the unconsolidated sedimentary material is a net loss. The southern region displays a large portion of the material being deposited back into this region (Figure 7).

4.3 Charles Pinckney National Historic Site

Areas near Charles Pinckney NHS experienced fluctuating elevations from 2007 to 2016. From 2010 to 2016, the elevation increased along the coastline and within the intercoastal waterway, while from 2016 to 2018 the elevation decreased along the coastline (Figure 8). Along this coastline the elevation changes that occurred were in many of the same areas. From 2010 to 2018 the areas representing the highest elevation remained constant as well as the areas with the lowest elevation. Though much of the area remained constant, the data represent areas that both decreased and increased in elevation along the coastline (Figure 8).

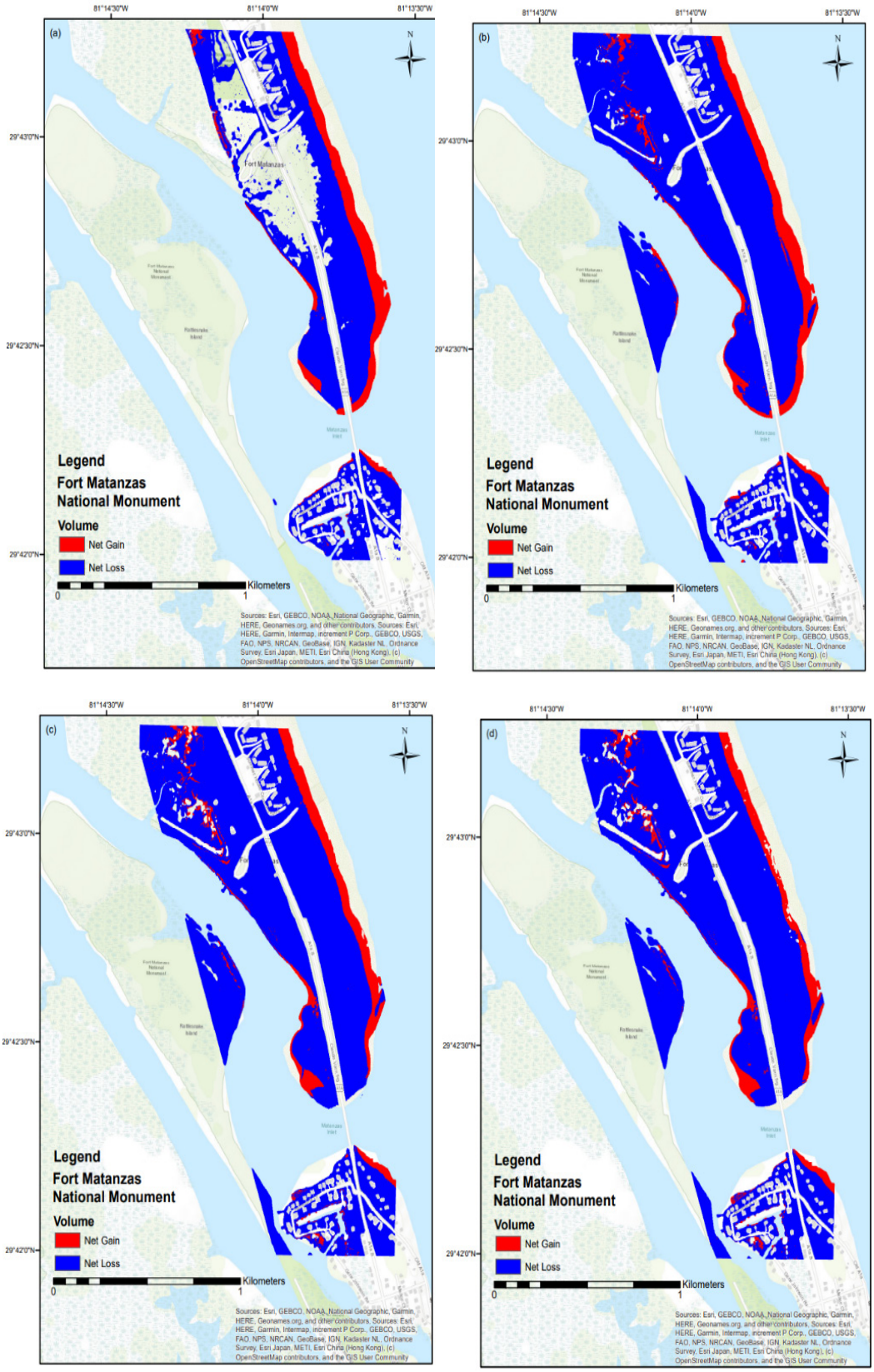

Figure 5. Spatial change maps detailing the volumetric distribution changes of both deposited (net gain) and erosional activity (net loss) of unconsolidated sedimentary material at Fort Matanzas NM from 2010 to 2017. Each panel corresponds to the specified year: (a) 2010, (b) 2013, (c) 2016, and (d) 2017.

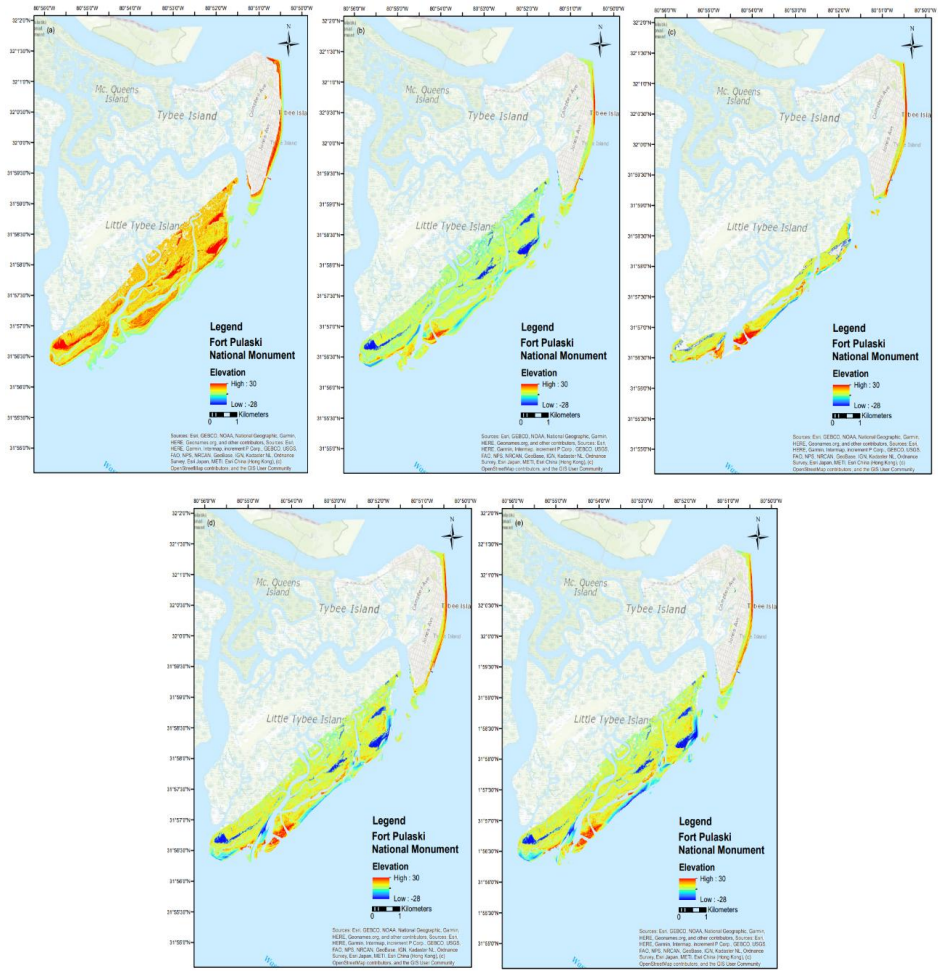

Figure 6. LiDAR derived DEM difference maps generating three-dimensional elevation changes of the area near Fort Pulaski NM from 2006 to 2017. Each panel corresponds to the specified year: (a) 2006, (b) 2009, (c) 2010, (d) 2016, and (e) 2017.

Table 3. Spatial change extent of sedimentary material deposited (net gain) and areas where erosional activity occurred (net loss).

SAVANNAH COAST SPATIAL CHANGE ANALYSIS		
	2009	
Total Area (m^2)	1,018,432	100%
Net Loss	870,192	85%
Net Gain	148240	15%
	2010	
Total Area (m^2)	377,555	100%
Net Loss	284,050	75%
Net Gain	93,504	25%
	2016	
Total Area (m^2)	931,287	100%
Net Loss	785,213	84%
Net Gain	146,074	16%
	2017	
Total Area (m^2)	964,442	100%
Net Loss	812,018	84%
Net Gain	152,423	16%

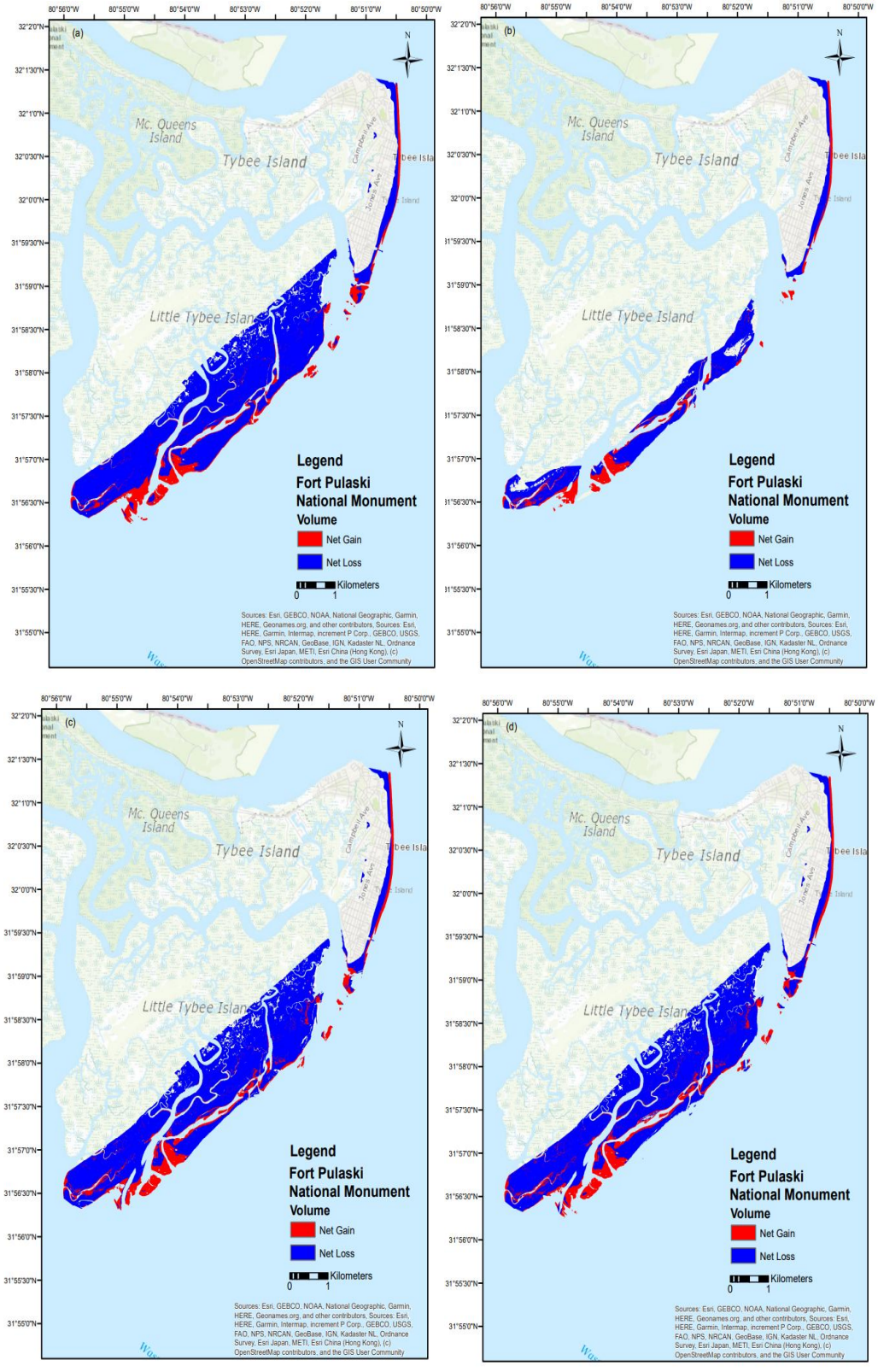

Figure 7. Spatial change maps detailing the volumetric distribution changes of both deposited (net gain) and erosional activity (net loss) of unconsolidated sedimentary material at Fort Pulaski NM from 2009 to 2017. Each panel corresponds to the specified year: (a) 2009, (b) 2010, (c) 2016, and (d) 2017.

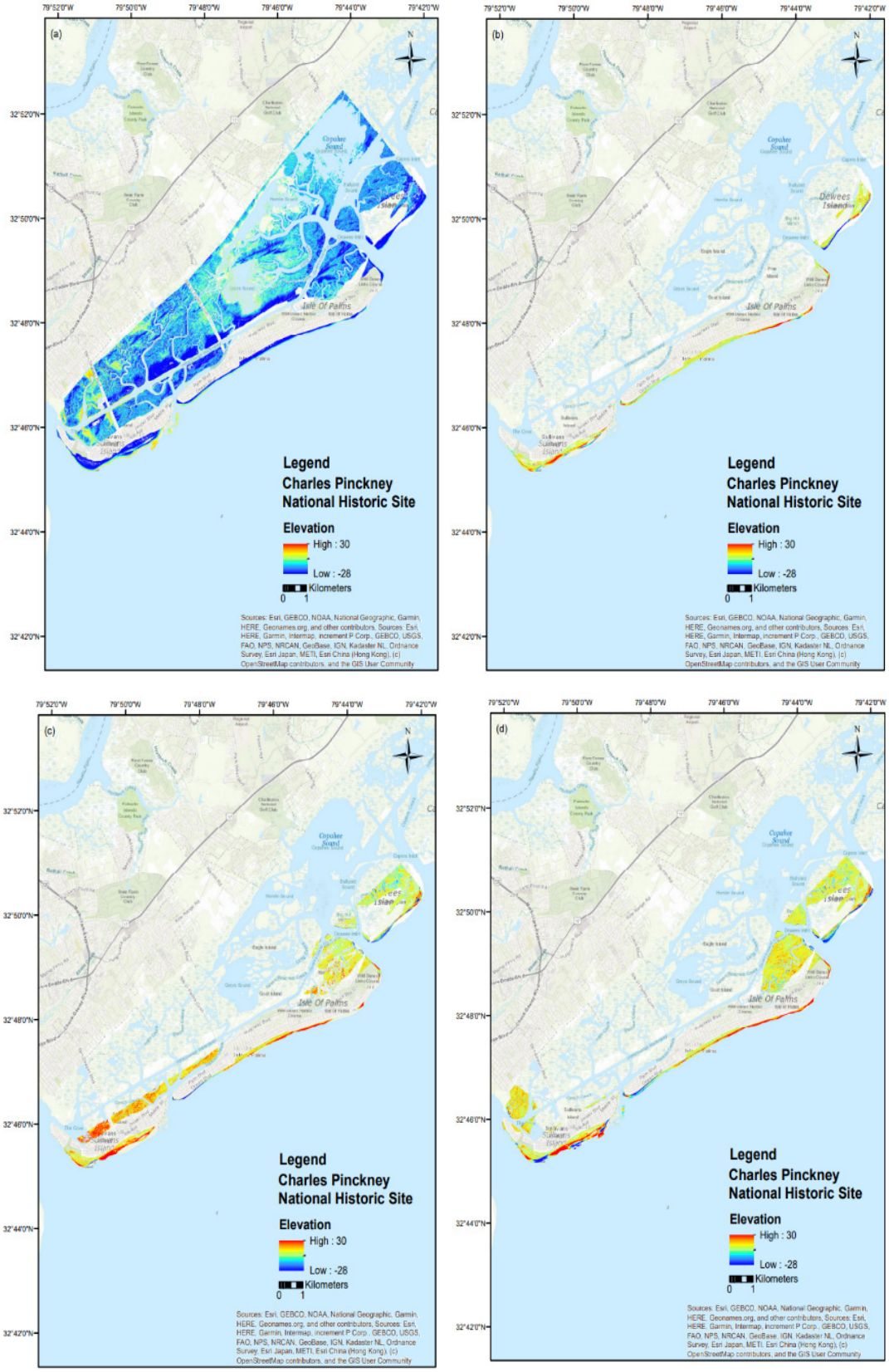

Figure 8. LiDAR derived DEM difference maps generating three-dimensional elevation changes of the area near Charles Pinckney NHS from 2007 to 2018. Each panel corresponds to the specified year: (a) 2007, (b) 2010, (c) 2016, and (d) 2018.

The volumetric change maps inform us that even though there is an overall net loss of unconsolidated sedimentary material, the volume fluctuated between 2010 to 2018 (Table 4). In 2010, erosional activity occurred at approximately 89%, decreased to 87% in 2016, and then increased to 89% in 2018. This suggests the unconsolidated sedimentary material fluctuated between a net gain and loss (Figure 9). The net gain is mostly in the southernmost region, while also visible in the tidal inlets near the Isle of Palms (Figure 9).

4.4 Cape Lookout National Seashore

The LiDAR derived DEMs of Cape Lookout NS depict a coastal environment that has continuously changed from 2012 to 2018. Elevations decreased from 2012 to 2014, increased from 2014 to 2016, and decreased from 2016 to 2018 (Figure 10). The difference maps also display areas along the coastline where the lowest elevation (western coastline) values remain constant along with the areas of higher elevation (eastern coastline) (Figure 10). The center of this coastal environment displayed topography that remained nearly consistent.

The volumetric change maps of Cape Lookout NS display a majority net loss of unconsolidated sedimentary material. The spatial change analysis shows how erosional activity decreased from 2014 to 2016, but then increased in 2018 (Table 5). This coastal environment displays that most of the erosional activity occurring is around the coastline, while the unconsolidated sedimentary material being deposited back into this environment is more inland (Figure 11). Noticeably, there is a drastic change from 2014 to 2016, where the inland portions of this region shifted from a net loss to a net gain (Figure 11). This depiction indicates how coastal environments can change over time. The volumetric distribution along the coastline shows a net gain, while the majority is a net loss. Identification of differences in the unconsolidated sedimentary material of this coastline is evident from 2014 to 2018. The inland portions of this region experienced the most change spatially. From 2014 to 2016, there was an increase of 47% of unconsolidated sedimentary material deposited back into this region, but in 2018 the volumetric distribution changed, resulting in a net loss of 60% (Table 5).

Table 4. Spatial change extent of sedimentary material deposited (net gain) and areas where erosional activity occurred (net loss).

SULLIVAN'S ISLAND COAST SPATIAL CHANGE ANALYSIS		
	2010	
Total Area (m^2)	242,790	100%
Net Loss	217,203	89%
Net Gain	25,587	11%
	2016	
Total Area (m^2)	672,972	100%
Net Loss	587,863	87%
Net Gain	85,109	13%
	2018	
Total Area (m^2)	846,323	100%
Net Loss	755,791	89%
Net Gain	90,532	11%

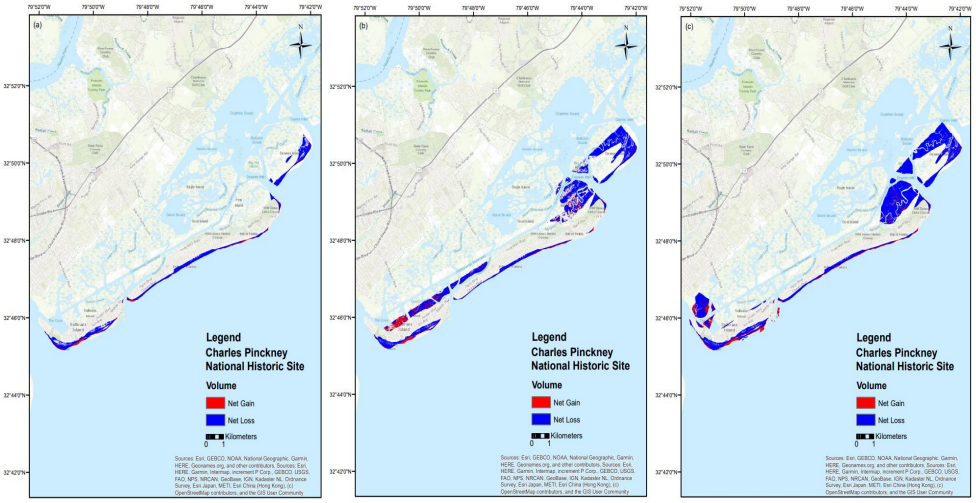

Figure 9. Spatial change maps detailing the volumetric distribution changes of both deposited (net gain) and erosional activity (net loss) of unconsolidated sedimentary material at Charles Pinckney NHS from 2010 to 2018. Each panel corresponds to the specified year: (a) 2010, (b) 2016, and (c) 2018.

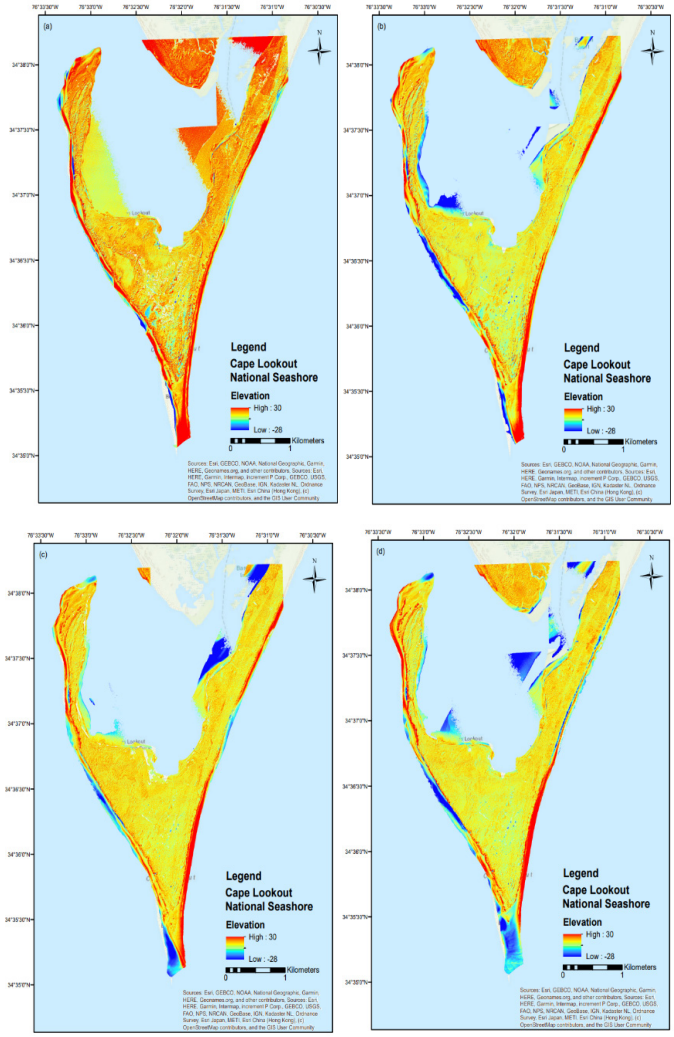

Figure 10. LiDAR derived DEM difference maps generating three-dimensional elevation changes of Cape Lookout NS from 2012 to 2018. Each panel corresponds to the specified year: (a) 2012, (b) 2014, (c) 2016, and (d) 2018.

Table 5. Cape Lookout NS spatial change extent of sedimentary material deposited (net gain) and areas where erosional activity occurred (net loss).

CAPE LOOKOUT NATIONAL SEASHORE SPATIAL CHANGE ANALYSIS		
	2014	
Total Area (m^2)	594,181	100%
Net Loss	449,294	76%
Net Gain	144,886	24%
	2016	
Total Area (m^2)	638,251	100%
Net Loss	337,810	53%
Net Gain	300,440	47%
	2018	
Total Area (m^2)	605,340	100%
Net Loss	363,235	60%
Net Gain	242,105	40%

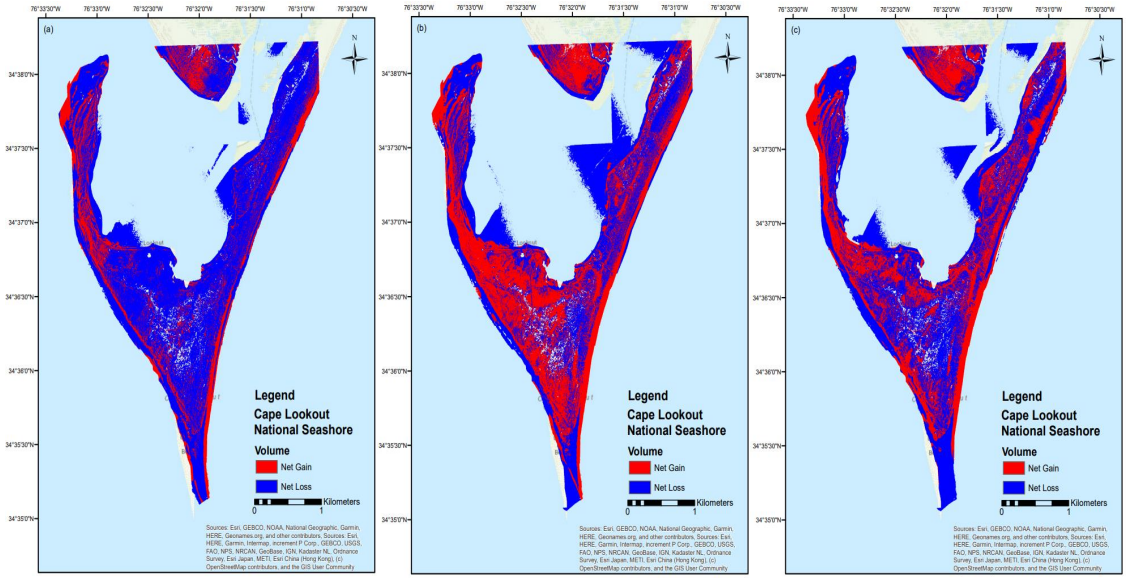

Figure 11. Spatial change maps detailing the volumetric distribution changes of both deposited (net gain) and erosional activity (net loss) of unconsolidated sedimentary material at Cape Lookout NS from 2014 to 2018. Each panel corresponds to the specified year: (a) 2014, (b) 2016, and (c) 2018.

5. Discussion

The coastal southeastern US has experienced the effects of sea level rise, storm frequency, and changes in climatic regimes that have caused this coastal region to be unstable. The steadily climbing sea level and increases in storm activity and intensity, threaten these coastal zones by making them susceptible to extreme flooding events, inundation, and erosion. These changes were demonstrated in this study using LiDAR at selected SECN NPS sites along the southeastern USA (Figures 4-11). Results indicated that though erosional activity was present, there was a net gain of sedimentary material returned within the sites (Figures 5, 7, 9, 11). Temporal erosion and longshore transport of sediment are results of the ever-changing climate producing storm surges and relative sea level rise.

Spatially distributed erosion occurred from 2006-2018 at each of the sites. In the data presented, Fort Matanzas NM displayed a steady decline in net gain of unconsolidated sedimentary material, while the areas near Fort Pulaski NM, Charles Pinckney NHS and Cape Lookout NS display how the geomorphology is steadily oscillating between erosional and depositional processes (Tables 2-5). It is clear the sediment budget of each of these coastal sites can

change in response to fluctuations of coastal depositional and erosional processes. The erosion that is occurring is in response to relative sea level and changes in climatic regimes, but what is most important is that these causes represent the quasi-cyclic phenomena [50,51]. This phenomenon represents how the unconsolidated sediment distribution and morphodynamic equilibrium change from the influence of fluctuating climatic regimes. These processes are not just exclusive to the coastal southeastern US but are found in other regions as well [52,53]. As the variability and frequency of these events continue, the impact of longshore transport on these coastal zones is unforeseen.

Throughout the study period, unconsolidated sedimentary material was either eroded or deposited at these SECN NPS sites, however there was an overall net gain. This is most notable along the coastlines (Figures 5, 7, 9, 11) where eroded areas had new material deposited causing the overall net gain. There are multiple processes that can cause this coastal morphodynamics, however, longshore sediment transport is evident. Longshore sediment transport depends on many factors, but the direction and speed of the longshore current primarily depend on the direction and height of the wave energy. Though these are highly variably, and the wave energy is dependent on the transport gradient under varying wave conditions, the sites indicate this process is plausible (Figures 5, 7, 9). For example, Cape Lookout NS shows longshore currents have caused repeated oscillation of eroded and deposited sediments under various conditions [54]. Previous studies at Cape Lookout NS have shown evidence of longshore sediment transport just as the findings of this study [55].

Along the coastal southeastern US, storm surges pose an imminent threat to coastal geomorphology. In 2016 a Category 5 hurricane, Hurricane Matthew, occurred in the coastal southeastern US causing inundation from precipitation in a geologically unstable coastal zone [56]. Post-Hurricane Matthew LiDAR datasets from this study show the impact of such hurricanes (Figures 5, 9, 11). The amplitude of the storm surge created the abnormal rise of sea level by wind energy. The wind energy produced strong tides and currents causing coastal erosion to increase. Erosional activity and longshore sediment transport events changed the volumetric distribution of unconsolidated sedimentary material of the coastal zone.

These elevational changes demonstrate how change in the land surface can impact the coastal hydrogeologic framework. Coastal recharge and discharge drainage networks can be altered with changes in sedimentary material [56]. Within this coastal zone there are both shallow and deep aquifers, thus, each respond differently [33,36,37,42,44-47,57]. The shallow aquifers are more responsive to the immediate climatic regimes, while the deeper aquifers have a delayed reaction. However, each aquifer is important as they each contribute to the coastal groundwater system of the coastal southeastern US.

5.1. Efficacy of Airborne LiDAR

LiDAR serves as a critical tool in understanding temporal and spatial topographic changes in the coastal southeastern US. LiDAR offers capabilities that allow researchers the opportunity to acquire large-scale elevation and derived topographic data for interpretation. The performance of the 3D laser scanners has advanced the speed and accuracy of assessing geomorphological changes within these coastal zones (Figures 4-11). The 3D lasers can take millions of precise measurements by examining the earth's topographical features through volume and elevation [21,58]. This ability highlights the success and scientific merit of observing the elevation and volumetric changes occurring in this study. The high accuracy and relative surface reflectance to define the topographic features are key in understanding erosional activity and where unconsolidated sediment is being deposited.

The defined topographic features are in part due to LiDAR's capabilities, while also using an appropriate ground truth validation technique to identify coastal changes. Through ENVI LiDAR, point cloud classification was applied to identify each class feature determined by the value of elevation height. These class features provide the capability to extract the necessary data related to various features on the surface. Point cloud classification displays the ability to be an appropriate approach to ground truth validation for the extraction of ground features representative of the earth's surface. This capability removed all roads, bridges, and buildings to accurately represent each region's surface. This technique will assist in providing accurate resource management to future studies on coastal environments [20-23,26,57,58].

Although more investigations are needed to understand the geomorphological changes that are occurring temporally and spatially, the remote sensing techniques used are advantageous. (1) Observations and investigations were performed remotely using available public domain datasets. (2) Surface data represented high sample density while not being affected by extreme weather conditions. (3) Data were acquired inaccessible areas with no geometric distortions. (4) The vast datasets provide the opportunity to identify relationships and new insights to better understand these coastal zones. The remote sensing techniques used through the acquisition of temporal LiDAR provided an appropriate representation of the geomorphological changes occurring [20-26].

5.2 Limitations and Applicability

This study provides sound results in distinctively describing the geomorphology of the coastal southeast US, along with some limitations that provide an opportunity for further research. First, the temporal LiDAR datasets aren't collected at the same time. This is important because the time in which the climatic regimes persist per unit area must be accounted for to characterize and understand which processes are occurring in an entire coastal zone. Second, under certain conditions elevation errors can occur while on water surfaces. This can produce a return value that is unreliable due to the height of the water depth affecting the reflection of the pulses. These errors are corrected by vertical and horizontal accuracy when using a standard method to compute the root mean square error (RMSE). Vertical accuracy is assessed by the fundamental accuracy value calculated at the 95th percentile confidence level as a function of the RMSE. The 95th percentile indicates that 95 percent of the errors in the dataset have absolute values of equal or lesser value, while 5 percent of the errors will be of larger value. Thus, there is approximately a 5 percent error. In suspected inundated areas where there was no return signal, no interpolation was applied. ENVI will interpolate the elevation data for missing data, however, this interpolation can result in false readings. Lastly, access to LiDAR data is limited. The temporal LiDAR data acquired for Fort Matanzas NM and Cape Lookout NS were in the SECN site boundaries, however, data acquired for Fort Pulaski NM and Charles Pinckney NHS were not in the SECN site boundary. The LiDAR data presented represented an area in the vicinity of the Fort Pulaski NM and Charles Pinckney NHS SECN site boundaries. The quality of this study is not only relevant to the advancement of understanding the coastal dynamic response, but it also presents efficient results with limited LiDAR derived datasets over the selected sites [21,57,58].

6. Conclusions

The southeast of the US is composed of numerous SECN NPS sites and each has experienced coastal changes. Outlined in this paper, Fort Matanzas NM, the area near Fort Pulaski NM, the area near Charles Pinckney NHS, and Cape Lookout NS, were analyzed to understand the geomorphologic changes occurring through the acquisition of temporal LiDAR derived datasets. These sites represented a portion of the coastal southeastern US to display the usefulness and versatility of processed LiDAR. Identifying the temporal changes in elevation and quantifying the spatial volumetric changes of unconsolidated sedimentary material allows for further understanding of the coastal dynamic response of the coastal southeast. This temporal and spatial change analysis displayed the vulnerability of these coastal zones due to elevation changes. In some cases, the elevation changes occur rapidly, but in other cases they occur over extended periods. Fort Matanzas NM displayed a 1-meter decrease in elevation from 2006 to 2017. Also, these elevation changes fluctuate causing these coastal zones to be unstable, presenting the opportunity for continuous change. Fort Matanzas NM elevation increased from 2010 to 2013 but decreased from 2016 to 2017 along the coastline. Fort Pulaski NM elevation increased from 2009 to 2010 and decreased in 2016. Charles Pinckney NHS elevation increased by 1-meter from 2010 to 2016 and decreased by 1-meter between 2016 to 2018. Cape Lookout NS elevation increased from 2012 to 2014, decreased from 2014 to 2016 and decreased from 2016 to 2018 on a magnitude of 2-3 meters. With respect to the coastal sediment budget, the volumetric spatial change of sedimentary material responded in conjunction with the elevation changes, however, the changes were not consistent. In areas in which there was a net gain/net loss of returned sedimentary material, the elevation increased and in areas where there was a net loss/net gain displaying erosional activity, the elevation decreased. Fort Matanzas NM displayed a 7% increase in erosional activity from 2010 to 2013, 1% increase from 2013 to 2016, and a 1% increase from 2016 to 2017. From 2009 to 2010 erosional activity in Fort Pulaski NM decreased by 10% but increased by 9% in 2016. Charles Pinckney NHS erosional activity decreased by 2% from 2010 to 2016 but increased in 2018 by 2%. Cape Lookout NS erosional activity decreased by 23% from 2014 to 2016 but increased in 2018 to 60%. These volumetric changes infer the climatic regimes that are persisting in the southeast US expose these coastal zones to instability. The quasi-cyclic phenomena that are occurring are due to these coastal zones being exposed to fluctuating climate regimes. As a result, there are different erosional processes and longshore sediment transport affecting the coastal hydrogeological and geomorphological dynamic.

The use of processed LiDAR derived data has furthered the understanding of coastal environments. The ability to use remote sensing techniques has offered the opportunity to identify the changes in geomorphology and its relationship with the climatic regime effects. As technology advances, new tools emerge, and more datasets are produced, the high-resolution data will improve coastal water resources and their applicability in providing sustainability and resiliency of coastal geomorphological change.

Author Contributions

David F. Richards, IV is the principal author of this manuscript and was responsible for the design, processing, interpretation, and writing of the manuscript. Adam M. Milewski made significant contributions to the design, processing, interpretation, writing, and review of the manuscript. Brian Gregory helped with the design, interpretation, and review of the manuscript.

Conflict of Interest

The authors declare no conflict of interest.

Funding

This work was funded by the National Park Service under cooperative agreement award: P17AC01646. Also, partially supported by the SEGS 2019 Student Research/ Field Work Grant and the NSF/GSA Graduate Student Geoscience Grant # 13005-20, which is funded by NSF Award # 1949901.

References

[1] Gornitz, V.M., Daniels, R.C., White, T.W., et al., 1994. The development of a coastal risk assessment database: vulnerability to sea level rise in the U.S. Southwest. Journal of Coastal Research Special Issue. 12, 327-338. http://www.jstor.org/stable/25735608.

[2] Wu, S.Y., Yarnal, B., Fisher, A., 2002. Vulnerability of coastal communities to sea-level rise: A case study of Cape May county, New Jersey, USA. Climate Research. 22(3), 255-270.

[3] Church, J.A., Hunter, J.R., McInnes, K.L., et al., 2006. Sea-level rise around the Australian coastline and the changing frequency of extreme sea-level events. Australian Meteorological Magazine. 55(4), 253-260.

[4] Leatherman, S.P., 1984. Coastal geomorphic response to sea level rise: Galveston Bay, Texas. Barth and Titus (eds). Coastal Zone. 151-178.

[5] Nicholls, R.J., Wong, P.P., Burkett, V., et al., 2007. Coastal systems and low-lying areas. https://ro.uow.edu.au/scipapers/. 164, 315-356.

[6] Markewich, H.W., Pavich, M.J., Buell, G.R., 1990. Contrasting soils and landscapes of the Piedmont and Coastal Plain, eastern United States. Geomorphology. 3(3-4), 417-447.
DOI: https://doi.org/10.1016/0169-555X(90)90015-I

[7] Leece, S.A., Pease, P.P., Gares, P.A., et al., 2006. Seasonal controls on sediment delivery in a small coastal plain watershed, North Carolina, USA. Geomorphology. 73 (3-4), 246-260.
DOI: https://doi.org/10.1016/j.geomorph.2005.05.017

[8] Philips, J.D., Wyrick, M., Robbins, J.G., et al., 1993. Accelerated erosion on the North Carolina coastal plain. Physical Geography. 14(2), 114-130.
DOI: https://doi.org/10.1080/02723646.1993.10642471

[9] Hauer, M.E., Evans, J.M., Mishra, D.R., 2016. Millions projected to be at risk from sea-level rise in the continental United States. Nature Climate Change. 6(7), 691-695.
DOI: https://doi.org/10.1038/nclimate2961

[10] Desmet, K., Kopp, R.E., Kulp, S.A., et al., 2018. Evaluating the economic cost of coastal flooding (No. w24918). National Bureau of Economic Research.
DOI: https://doi.org/10.3386/w24918

[11] Klein, R.J.T., Nicholls, R.J., 1999. Assessment of coastal vulnerability to climate change. Ambio. pp. 182-187. https://www.jstor.org/stable/4314873.

[12] Lindsey, R., 2019. Climate Change: Global Sea Level. National oceanic and atmospheric administration (NOAA), National Ocean Service, Silver Spring. https://www.climate.gov/news-features/understanding-climate/climate-change-global-sea-level (Accessed on 18 January 2020).

[13] Bamber, J.L., Oppenheimer, M., Kopp, R.E., et al., 2019. Ice sheet contributions to future sea-level rise from structured expert judgment. Proceedings of the National Academy of Sciences. 116(23), 11195-11200.
DOI: https://doi.org/10.1073/pnas.1817205116

[14] Von Holle, B., Irish, J.L., Spivy, A., et al., 2019. Effects of future sea level rise on coastal habitat. Journal of Wildlife Management. 83(3), 694-704.
DOI: https://doi.org/10.1002/jwmg.21633

[15] Morton, R.A., 2003. An overview of coastal land loss: With emphasis on the southeastern United States. United States (p. 28). US Geological Survey, Center for Coastal and Watershed Studies. https://citeseerx.ist.psu.edu/viewdoc/download?-doi=10.1.1.730.5008&rep=rep1&type=pdf.

[16] Morton, R.A., Miller, T.L., 2005. National assessment of shoreline change: Part 2, Historical shoreline change and associated land loss along the U.S. Southeast Atlantic coast. U.S. Geological Survey. Open-File Report. 1401, 1-40.
DOI: https://doi.org/10.3133/ofr20051401

[17] Gutierrez, B.T., Plant, N.G., Thieler, E.R., 2011. A Bayesian network to predict coastal vulnerability to sea level rise. Journal of Geophysical Research: Earth Surface. 116(F2).
DOI: https://doi.org/10.1029/2010JF001891

[18] Brock, J.C., Purkis, S.J., 2009. The emerging role of lidar remote sensing in coastal research and resource management. Journal of Coastal Research. (10053), 1-5.
DOI: https://doi.org/10.2112/SI53-001.1

[19] Carson, W.W., Anderson, H.E., Reutebuch, S.E., et al., 2004. May. LiDAR applications in forestry – An overview. Proceedings of the American Society of Photogrammetry and Remote Sensing Annual Conference (pp. 1-9) 04-1-2-02_04_1_2_02_deliverable_06.pdf (firescience.gov).

[20] Sallenger, A.H., Jr., Krabill, W.B., Swift, R.N., et al., 2003. Evaluation of airborne topographic lidar for quantifying beach changes. Journal of Coastal Research. 125-133. https://www.jstor.org/stable/4299152.

[21] Woolard, J.W., Colby, J.D., 2002. Spatial characterization, resolution, and volumetric change of coastal dunes using airborne LIDAR: Cape Hatteras, North Carolina. Geomorphology. 48(1-3), 269-287.
DOI: https://doi.org/10.1016/S0169-555X(02)00185-X

[22] Young, A.P., Ashford, S.A., 2006. Application of airborne lidar for seacliff volumetric change and beach-sediment budget contributions. Journal of Coastal Research. 22(2), 307-318.
DOI: https://doi.org/10.2112/05-0548.1

[23] O'Dea, A., Brodie, K.L., Hartzell, P., 2019. Continuous coastal monitoring with an automated terrestrial lidar scanner. Journal of Marine Science and Engineering. 7(2), 37.
DOI: https://doi.org/10.3390/jmse7020037

[24] Gesch, D.B., 2009. Analysis of lidar elevation data for improved identification and delineation of lands vulnerable to sea-level rise. Journal of Coastal Research. 53, 49-58.
DOI: https://doi.org/10.2112/SI53-006.1

[25] Elaksher, A., 2008. Fusion of hyperspectral images and lidar-based dems for coastal mapping. Optics and Lasers in Engineering. 46(7), 493-498.
DOI: https://doi.org/10.1016/j.optlaseng.2008.01.012

[26] Titus, J.G., Richmond, C., 2001. Maps of lands vulnerable to sea level rise: modeled elevations along the US Atlantic and Gulf coasts. Climate Research. 18(3), 1-24.
DOI: https://doi.org/10.3354/cr018205

[27] Barnhardt, W., Denny, J., Baldwin, W., et al., 2007. Geologic framework of the Long Bay inner shelf: implications for coastal evolution in South Carolina. Coastal Sediments. 2151-2160.
DOI: https://doi.org/10.1061/40926(239)169

[28] Warner, J.C., Armstrong, B., Sylvester, C.S., et al., 2012. Storm-induced inner-continental shelf circulation and sediment transport: Long Bay, South Carolina. Continental Shelf Research. 42, 51-63.
DOI: https://doi.org/10.1016/j.csr.2012.05.001

[29] Ingram, K., Dow, K., Carter, L., et al., 2013. Climate of the southeast United States: Variability, change, impacts, and vulnerability. Washington DC; Island Press/Center for Resource Economics.

[30] Davey, C.A., Redmond, K.T., Simeral, D.B., 2007. Weather and Climate Inventory, National Park Service, Southeast Coast Network. Natural Resource Technical Report NPS/SECN/NRTR- 2007/010. National Park Service, Fort Collins, Colorado.

[31] Phillips, J.D., 1997. A short history of a flat place, three centuries of geomorphic change in the Croatan. Annals of the Association of American Geographers. 87(2), 197-216.
DOI: https://doi.org/10.1111/0004-5608.872050

[32] Campbell, K.M., Rupert, F.R., Arthur, J.D., et al., 2001. Geologic map of the state of Florida. Tallahassee, FL: Florida Geological Survey.

[33] Faulkner, G.L., 1970. Geohydrology of the Cross-Florida Barge Canal area with special reference to the Ocala vicinity. Diane Publishing.

[34] Graham, J., 2009. Geologic resources inventory scoping summary Fort Matanzas National Monument, Florida. Geologic resources Division National Park Service U.S. Department of the Interior. 1-9.

[35] Tibbals, C.H., 1990. Hydrology of the Floridan aquifer system in east-central Florida. U.S. Geological Survey Professional Paper; (USA).

[36] Clarke, J.S., Hacke, C.M., Peck, M.F., 1990. Geology and ground water resources of the coastal area of Georgia. Bulletin (USA).

[37] Weems, R.E., Edwards, L.E., 2001. Geology of Oligocene, Miocene and Younger deposits in the coastal area of Georgia (Vol. 131). Department of Natural Resources, Environmental Protection Division, Georgia Geologic Survey.

[38] Veatch, O., Stephenson, L.W., 1911. Preliminary report on the geology of the Coastal Plain of Georgia (No. 26). Foote & Davies Company.

[39] Huddleston, P.F., 1988. A revision of the lithostratigraphic units of the Coastal Plain of Georgia: The Miocene through Holocene. Georgia Geological Survey, Bulletin. 105, 1-152. B-104.pdf (georgia.gov).

[40] Heron, S.D., Robinson, G.D., Johnson, H.S., Jr., 1965. Clays and opal-bearing claystones of the South Carolina Coastal Plain (No. 31). State Department Board.

[41] Sloan, E., 1979. Catalogue of the mineral localities of

South Carolina. South Carolina Geological Survey.

[42] Campbell, B.G., 1996. Geology, hydrogeology, and potential of intrinsic bioremediation at the National Park Service Dockside II site and adjacent areas, Charleston, South Carolina, 1993-94 (Vol. 96, No. 4170). US Geological Survey.

[43] Aucott, W.R., Davis, M.E., Speiran, G.K., 1987. Geohydrologic framework for the Coastal Plain aquifers of South Carolina (No. 85-4271).

[44] Aucott, W.R., 1996. Hydrology of the Southeastern Coastal Plain aquifer system in South Carolina and parts of Georgia and North Carolina (No. 1410-E). U.S. Geological Survey.
DOI: https://doi.org/10.3133/pp1410E

[45] Aucott, W.R., 1988. The predevelopment groundwater flow system and hydrologic characteristics of the Coastal Plain aquifers of South Carolina (Vol. 86, No. 4347). US Department of the Interior, U.S. Geological Survey.

[46] Lautier, J.C., 2001. Hydrogeologic framework and groundwater conditions in the North Carolina Central Coastal Plain. North Carolina Department of Environment and Natural Resources Division of Water Resources.

[47] Winner, M.D., 1978. Ground-water resources of the Cape Lookout National Seashore, North Carolina (No. 78-52) U.S. Geological Survey, Raleigh, North Carolina. 78-52, 1-59.

[48] Lautier, J.C., 2009. Hydrogeologic framework and groundwater conditions in the North Carolina East Central Coastal Plain. North Carolina Department of Environment and Natural Resources Division of Water Resources.

[49] NOAA: Data Access Viewer. n.d. National Oceanic and Atmospheric Administration (NOAA), NOAA Office of Coastal Management. https://coast.noaa.gov/dataviewer/#/lidar/search/ (Accessed on 3 May 2018).

[50] Ranasinghe, R., 2016. Assessing climate change impacts on open sandy coasts: A review. Earth Science Reviews.160, 320-332.
DOI: https://doi.org/10.1016/j.earscirev.2016.07.011

[51] Clarke, D.J., Eliot, I.G., 1987. Groundwater level changes in a coastal dune, sea-level fluctuations and shoreline movement on a sandy beach. Marine Geology. 77(3-4), 319-326.
DOI: https://doi.org/10.1016/0025-3227(87)90120-4

[52] Aubrey, D.G., 1983. Beach changes on costs with different wave climates. Sandy beaches as ecosystems. pp. 63-85.

[53] Vousdoukas, M.I., Ranasinghe, R., Mentaschi, L., et al., 2020. Sandy coastlines under threat of erosion. Nature Climate Change. 10(3), 260-263.
DOI: https://doi.org/10.1038/s41558-020-0697-0

[54] Park, J.Y., Wells, J.T., 2005. Longshore transport at Cape Lookout, North Carolina: shoal evolution and the regional sediment budget. Journal of Coastal Research. 21(1), 1-17.
DOI: https://doi.org/10.2112/02051.1

[55] Park, J.Y., Wells, J.T., 2005. Longshore transport at Cape Lookout, North Carolina: shoal evolution and the regional sediment budget. Journal of Coastal Research. 21(1), 1-17.
DOI: https://doi.org/10.2112/02051.1

[56] Leung, L.R., Prasad, R. 2019. Potential impacts of accelerated climate change: Third Annual Report of Work (No. PNNL-27452-Rev. 1). Paciffic Northwest National Lab. (PNNL), Richland, WA United States.
DOI: https://doi.org/10.2172/1524249

[57] Hoover, D.J., Odigie, K.O., Swarzenski, P.W., et al., 2017. Sea-level rise and coastal groundwater inundation and shoaling at select sites in California, USA. Journal of Hydrology: Regional Studies. 11, 234-249.
DOI: https://doi.org/10.1016/j.ejrh.2015.12.055

[58] Deronde, B., Houthuys, R., Henriet, J.P., et al., 2008. Monitoring of the sediment dynamics along a sandy shoreline by means of airborne hyperspectral remote sensing and LiDAR: a case study in Belgium. Earth Surface Processes and Landforms: The Journal of the British Geomorphological Research Group. 33(2), 280-294.
DOI: https://doi.org/10.1002/esp.1545